Article

An Analysis of Miscible Displacement and Numerical Modelling of Glyphosate Transport in Three Different Agricultural Soils

Kamrun Nahar [1],* and Robert K. Niven [2]

1   School of Agriculture and Environmental Science, University of Southern Queensland, Toowoomba, QLD 4350, Australia
2   School of Engineering and Technology, The University of New South Wales, Northcott Drive, Canberra, ACT 2600, Australia; r.niven@adfa.edu.au
*   Correspondence: kamrun.nahar@unisq.edu.au; Tel.: +61-7-4631-1733

Abstract: Since the introduction of genetically modified (GM) glyphosate-resistant crops, especially in Australia, the United States, and Canada, the use of glyphosate has exploded, raising concerns about its environmental effects both in terrestrial and aquatic environments. There are several factors that can affect the transport of glyphosate in soil, including the pH of the soil, the iron and aluminium oxides in the soil, and the structure of the soil, as well as the application time and microbial biodegradation in the soil. Furthermore, some field studies have shown that glyphosate, along with its degradation products, can be found deep in the aquatic environment and can contaminate groundwater by leaching, which implies that studying glyphosate leaching through agricultural soils is very crucial. The research in this study involves column-leaching experiments on glyphosate-dosed soils using application and flow rates representative of field conditions with bromide as a non-reactive tracer. To determine whether the observed behaviour of glyphosate is consistent with commonly recognized transport processes, the results obtained were incorporated into a one-dimensional transport model (HYDRUS 1D). Initially, physical transport parameters were determined by fitting experimental bromide breakthrough curves (BTCs) with analytical solutions to advection–dispersion equations (ADEs) for pulse boundary conditions at the upper end and zero-gradient conditions at the lower end. Then, these parameters and those from the sorption experiments were used in HYDRUS 1D to describe glyphosate transport behaviour. After three different glyphosate applications, the columns with soils C and A showed the highest glyphosate leaching rates, which is closely related to their macropore structures since bromide also leached at higher rates. A similar lower glyphosate leaching rate was found for soil B as for bromide BTC, indicating that competition between phosphorus and glyphosate for sorption sites did not result in higher rates of leaching.

Keywords: glyphosate; fate and transport; HYDRUS 1D; leaching; breakthrough curves

1. Introduction

Glyphosate (N-(phosphonomethyl) glycine) is an odourless, white, solid post-emergence herbicide used for controlling weeds in agriculture, forestry, and aquaculture. Monsanto first introduced it in 1971 as an unwanted weedkiller for agricultural purposes, and Table 1 summarizes its physical and chemical properties [1,2]. Several commercial products contain this active ingredient, including Roundup, widely used in genetically modified crops. In soil materials, glyphosate shows extreme solubility, mostly because of the presence of aluminium oxides and iron oxides in the compound, along with a low pH value [3–12]. The amount of glyphosate in soil has been shown to vary according to pH, iron and aluminium oxides, and soil structures as well as the timing and activity of glyphosate application [3,8,12–16]. A number of studies have also suggested that glyphosate could potentially be transported from terrestrial to aquatic environments as a sorbable compound in solution or in suspension, depending on the form in which it is formed [17–19]. By leaching through soil (subsurface

runoff), dissolved forms enter drainage and groundwater, whereas particle-bound forms are moved into open water bodies through overland flow (surface runoff) [14,20–22].

Table 1. Physical and chemical properties of glyphosate.

Active Ingredient	Log K_{ow}	K_{oc}	Henry's Constant (atm-m^3/mol)	Molecular Weight (g/mol)	Form	Vapour Pressure mPa (25 °C) or mmHg (45 °C)
Glyphosate acid	<-3.2	300–20,100	4.08×10^{-19}	169.07	Odourless, white solids	1.31×10^{-2} or 1.84×10^{-7}
Glyphosate isopro-pylamine salt	-3.87 or -5.4	300–20,100	6.27×10^{-27}	228.19	Odourless, white solids	2.1×10^{-3} or 1.58×10^{-8}
Glyphosate ammonium salt	-3.7 or -5.32	300–20,100	1.5×10^{-13}	186.11	Odourless, white solids	9×10^{-3} or 6.75×10^{-8}

In non-structured soils, such as sandy soils with high hydraulic conductivity that receive large amounts of precipitation, glyphosate can be transported more readily. There is a possibility that these soils can permit greater glyphosate leaching despite having a lower sorption capacity. In a previous study [23] it was found that sandy soils were at a high risk of glyphosate leaching due to their limited sorption capacity. There was no leaching of glyphosate (or its degradation product AMPA) when a further two years of field studies were conducted due to a lack of macropores, meaning the sandy soil had no structure, and water moved through it as if it were a piston flow [18].

The leaching of glyphosate in sandy soils without macropores was also reported by other studies [14–16]. Structured soils [17] with macropores can enhance pesticide transport rates, and glyphosate (and AMPA) has been reported to leach from subsurface sites [10–12]. Glyphosate leaching has been reported to be severe in gravelly soils with coarse textures [24,25].

This study investigates whether glyphosate can be released through macropore flows from GM canola agricultural soil with increased sorption capacities. This was accomplished by column leaching glyphosate-dosed soils using application and flow rates that reflect field conditions. To assess whether the experimental results are consistent with commonly accepted transport mechanisms, they were incorporated into an analysis of one-dimensional transport processes.

2. Materials and Methods

2.1. Reagents

In this study, glyphosate (PESTANAL, HPLC grade) and FMOC-Cl were obtained from Fluka (Dresden, Germany), and acetonitrile and diethylether from Sigma-Aldrich Australia (Melbourne, Australia). In addition to the diethylether, the other chemicals included KBr, KCl, HCl, KOH, NaOH, disodium tetraborate decahydrate ($Na_2B_4O_7 \cdot 10H_2O$), and potassium phosphate monobasic (KH_2PO_4), all of which were analytical grade.

2.2. Solutions

Experimental solutions were prepared by mixing glyphosate (PESTANAL, 99.729%) with distilled water as well as a background electrolyte (0.1M KCl). Before the experiments were conducted, FMOC-Cl solutions of 1 g L^{-1} were prepared by dissolving the reagent in acetonitrile. The buffer solution (pH = 9) was prepared by dissolving 15.255 g of $Na_2B_4O_7 \cdot 10H_2O$ in 1000 mL of distilled water. To correct samples' sensitivity to divalent ions in amino-acid coupling, samples were pre-treated with a 0.1 M EDTA solution [26]. KBr (0.01 M) solutions prepared in HPLC-grade water were used as non-adsorbed tracers in soil column experiments.

2.3. Soil Materials

In order to conduct the glyphosate leaching trial for a comparative analysis, soil samples were collected from three different locations of the investigated area. In a continuous cropping rotation, the land was used to grow winter cereals, canola, and legumes through the use of no-till and traffic-control practices to minimize soil erosion [27].

In order to fill the columns, three different soils were collected: soil A was collected from a field that had not been cultivated with genetically modified canola in the past five years, soil B was collected from a field that was just about to end canola harvesting, and soil C was collected from a field that had completed canola cultivation. Physico-chemical properties of the soil were determined using the standard methods presented in Table 2.

Table 2. Soil properties.

Soil Column	Bulk Density, g cm^{-3}	Irrigation Rate, cm h^{-1}	Pore-Water Velocity (v), cm h^{-1}	Dispersion Coefficient (D), cm^{2}d^{-1}	Soil Water Content (θ), cm^{3}cm^{-3}	pH	OC	CEC	Fe (%)	Al (%)	Sand (%)	Silt (%)	Clay (%)
Soil A	1.5	0.4	2.624	19.73	0.152	4.5	0.94	6.81	5.63	9.01	47.2	39	13.8
Soil B	1.5	0.4	2.488	14.64	0.160	4.8	1.1	7.4	17.59	14.2	43.2	29	27.8
Soil C	1.5	0.4	2.734	24.49	0.146	5	0.9	4.75	7.65	11.0	41.2	43	15.8

2.4. Experimental Studies on Column Leaching

2.4.1. The Experimental Setup

Three glass columns (5 cm inner diameter, 20 cm height) were filled with air-dried and sieved topsoil (up to 15 cm in depth and 1.5 g/cm^3) from three different agricultural sites (A, B, and C) and fitted with glass sinter plates on their bottoms. A Teflon tube (3 mm inner diameter) was connected to each outlet, and a leachate collector was placed below the glass sinter disc. Each column was equipped with a disc with 30 holes that was attached to a peristaltic pump with speed control, which was connected to a reservoir filled with water, as shown in Figure 1.
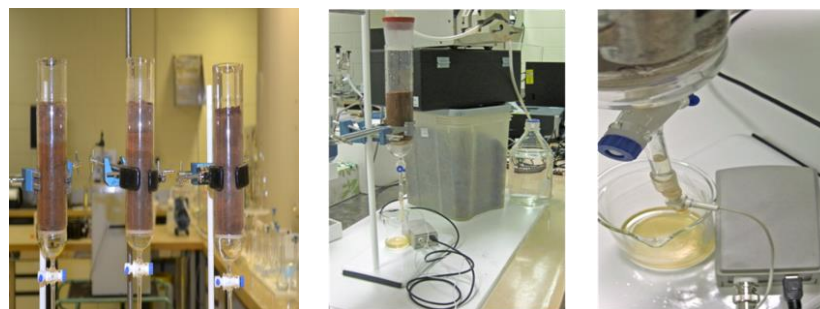
Figure 1. Column leaching experimental set-up.

To achieve steady-state hydrodynamic conditions that result in constant outflow, the columns were preconditioned for three days prior to application of the glyphosate solution. An application of glyphosate directly to the soil's surface was performed using a conventional spray head and a pulse application using syringes (50 mL). Analyses were conducted on effluent samples collected from the bottom of the column as they passed through the Teflon tube for glyphosate, bromide, pH, and electrical conductivity. At a temperature of 20 ($\pm$5) °C, the glyphosate concentrations in the leachate were measured using the UV–visible direct spectrophotometric method.

2.4.2. The Application of Glyphosate

As a small molecule with three polar functional groups (carboxyl, amino, and phosphonate), glyphosate is strongly sorbed by soil minerals after application [7,9,23,28–31]

and has a half-life of 3–174 days in soil minerals and 5–91 days in water [32]. Even though the carboxylic group can also contribute to glyphosate sorption in soil, it usually occurs through the phosphonic acid group (organic compounds that contain $C-PO(OH)_2$ or $C-PO(OR)_2$) [3,7,28,33,34]. Considering soil glyphosate contact time variations and soil phosphate accumulation, three different glyphosate applications were applied. Glyphosate applications were preceded by artificial rain (0.01 M $CaCl_2$), as recommended by the Environmental Protection Agency (EPA) [35]. The soil was irrigated with artificial rain (0.01 M $CaCl_2$) after application 1 of glyphosate, while applications 2 and 3 were applied evenly over a soil column's surface and left for three days before irrigation. During application 3, additional phosphorous (KH_2PO_4 (0.008 M)) was applied to the column in addition to the pre-saturation solution [27].

Using 50 mL syringes, potassium bromide (0.01 M) and glyphosate solutions were pulsed into each column (application 1). Following one hour of artificial rain, the glyphosate pulse application was followed by irrigation with rainwater for four hours, followed by the bromide pulse application using 0.01M KBr and KOH as a background electrolyte. A glyphosate application rate of 4.5 kg/ha was chosen based on realistic values according to the equation given in the EPA guidelines [24], with each column containing 10 L of Roundup, the highest of the recommended rates for farmland (2 to 10 L ha^{-1}) [35]. Three hours later, irrigation was continued, with its rate (4 ± 0.2 mm/h) chosen according to the highest rainfall occurring during the whole year of GM canola cultivation from sowing to harvesting. Column leachates were collected and analysed for bromide, glyphosate, pH, and electrical conductivity at different time intervals.

2.4.3. Column Experiments Parameters

HYDRUS 1D, a numerical model capable of simulating the movement of water and solutes in soil under both equilibrium and non-equilibrium flow and transport conditions, was used to model the miscible displacement experiments with glyphosate and bromide as a non-reactive tracer. Using finite-element methods, it solves the Richards equation for variable saturated fluid flows and advection–dispersion equations for heat and solute transports. Under steady-state conditions, where the columns were packed homogeneously and irrigated at a constant rate to maintain a homogeneous water content distribution, a numerical one-dimensional transport model was used to simulate the transport of solutes. A transport model was used to determine whether glyphosate's observed transport behaviour matched commonly recognized processes. In addition, an inverse model was used to estimate the reaction and transport parameters based on the model solution fitted to the observed data. This method involves iteratively changing the model parameters until the best-fit model solution is achieved using a least-squares optimization routine.

2.5. Bromide Transport

Fitting the experimental bromide BTCs with the analytical solution to the ADEs for pulse boundary conditions at the upper end and zero-gradient conditions at the lower end determined the physical transport parameters. CXTFIT [36] was used in the inverse mode with the ADE for an inert tracer and rewritten as follows:

$$\frac{\partial C}{\partial t} = D\frac{\partial^2 C}{\partial z^2} - v\frac{\partial C}{\partial z} \tag{1}$$

where C is the liquid phase concentration [M L^{-3}], *t* the time [T], D the dispersion coefficient [L^2 T^{-1}], z the depth [L], and v the pore-water velocity [L T^{-1}]. The parameters v and D were estimated and the dispersivity (λ) and volumetric water content (θ) calculated, respectively, as D/v and $\frac{j_w}{v}$, where j_w is the irrigation rate.

2.6. Glyphosate Transport

This study analysed the transport of glyphosate using a convective–dispersive model with degradation and kinetic sorption based on Equations (2) to (4). A simple equilibrium

model was used to predict glyphosate breakthrough based on parameters from the tracer experiment and K_f and n values from the batch experiment. This model has also been used in its inverse mode to fit glyphosate-equivalent BTCs with K_f and n. The one-site sorption model is described by the following system of equations:

$$\theta \frac{\partial C}{\partial t} + \rho \frac{\partial s^k}{\partial t} = \theta D \frac{\partial^2 C}{\partial z^2} - \theta v \frac{\partial C}{\partial z} - \mu C \qquad (2)$$

$$\rho \frac{\partial s^k}{\partial t} = \alpha_k \rho \left[s_e^k - s^k \right] - \mu C \qquad (3)$$

$$s_e^k = K_f C^n \qquad (4)$$

where s_e^k is the sorbed concentration that would be reached at equilibrium with the liquid phase concentration $[MM^{-1}]$, s^k the sorbed concentration of the kinetic sorption sites $[MM-1]$, ρ the soil's bulk density $[M\ L^{-3}]$, θ the water content $[L^3 L^{-3}]$, α_k a first-order sorption rate constant $[T^{-1}]$, μ a first-order dissipation rate $[T^{-1}]$, K_f the Freundlich sorption coefficients $[M^{1-(1/n)}L^n M^{-1}]$, and n the Freundlich exponent [-]. These four unknown parameters, α_k, μ, K_f, and n, were estimated by fitting the curve to the experimental data.

Simulations of solute transport were conducted with flux concentrations at the top and zero concentration gradients at the bottom. Assuming the same physical transport processes as those for bromide, the physical transport parameters for BTC (provided in Table 2) were taken from the solution of bromide BTC.

3. Results

3.1. Bromide Breakthrough Curves

As shown in Figure 2, the BTCs of the three different soil columns were determined by using a non-reactive tracer (bromide). The column with soil C had a faster bromide transport due to its higher pore-water velocity and lower water content in comparison with the other columns. The physical properties of these soil columns are provided in Table 2. The bulk densities (ρ) and irrigation rates (j_w) were determined experimentally, the pore-water velocities (v) and dispersion coefficients (D) fitted to the bromide BTCs (Figure 2). The BTCs of all three soil columns were well described by the physical equilibrium ADEs, with r^2 values of 0.99.


(**a**) Fitted data for soil A, soil B, and soil C. (**b**) Bromide concentration.
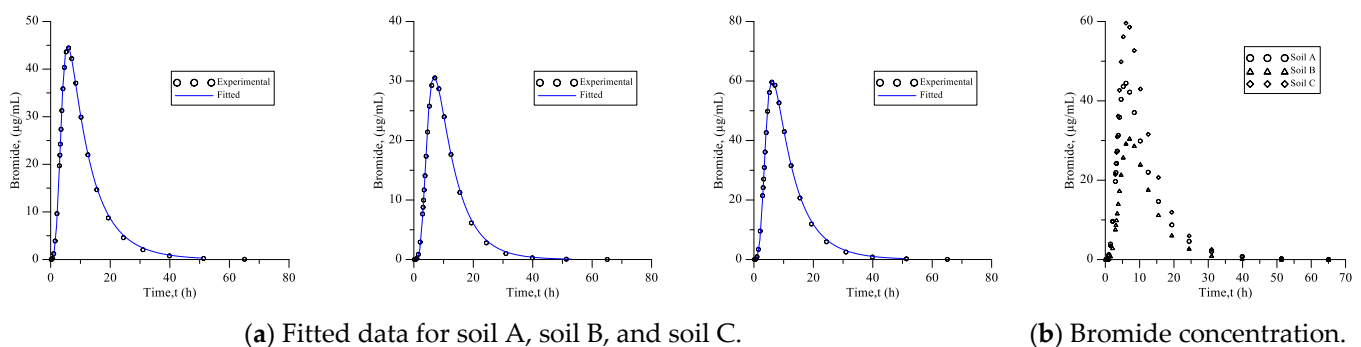
Figure 2. (**a**) Bromide breakthrough curves fitted with experimental data. (**b**) Bromide concentrations.

3.2. Glyphosate Breakthrough Curves

A, B, and C soil columns showed glyphosate breakthrough after 100 h, 312 h, and 103 h, respectively, following application 1. In soil column C, glyphosate breakthrough peaked at 0.7627 g/mL, consistent with soil C's lower sorption capacity than soils A and B (Figure 3). A, B, and C soils had their first arrivals of glyphosate after 205, 328, and 168 h, respectively, in leachate samples from glyphosate application 2. The role of phosphorus in the pre-saturation solution in the leaching of glyphosate was difficult to assess from the

present data for glyphosate application 3. The leaching rates of glyphosate were highest in columns with soils C and A, which was likely related to their macropore structures since bromide also leached more rapidly. Additionally, the leaching rates of glyphosate from soil B were similar to the leaching rates of its bromide BTC. It was found that the competition between phosphorus and glyphosate for sorption sites did not result in a higher leaching rate, despite the 3-day contact time between soil and solution. The results here contradict the results of previous batch sorption experiments, which showed a significant decrease in glyphosate sorption when KH_2PO_4 was present [3].

Application 1   Application 2   Application 3
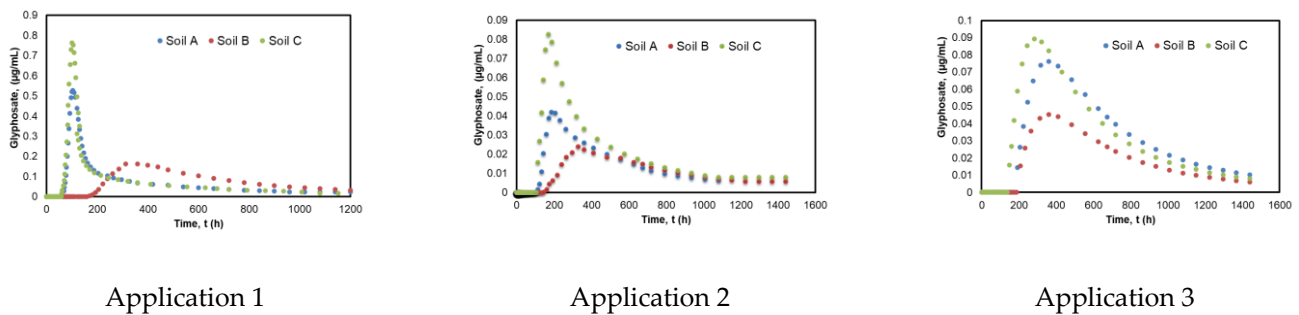
Figure 3. Glyphosate breakthrough curves under different application scenarios.

A number of studies found that glyphosate sorption by goethite decreases with increasing pH [37,38] similar to how other phosphonates and phosphate sorption decreases with increasing pH. Additionally, in uniform non-structured soils, such as sandy soils with high hydraulic conductivity and high precipitation rates, glyphosate leaching is prevented by lower sorption capacities. Based on a summary of the three soils, soil B had the lowest effluent glyphosate concentration, which was attributed to (1) lower breakthrough bromide concentrations, (2) lower pH values (Figure 4), and (3) higher electrical conductivity (Figure 4). Therefore, soil B had a lower glyphosate effluent concentration due to its lower pore-water velocity compared to soils A and C.
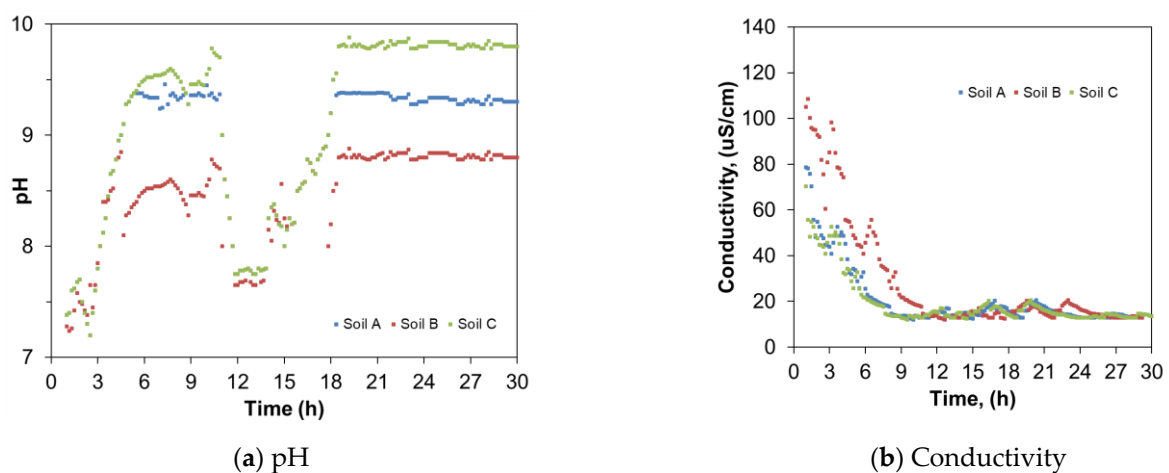
(**a**) pH   (**b**) Conductivity

**Figure 4.** pH and conductivity levels in effluent samples.

3.3. Mass Recovery

In addition to strong interactions with soils, glyphosate can be adsorbed on soils via relatively weak bonds, such as hydrogen bonds with soil humic material, so it is important to determine whether glyphosate can be desorbed from soils. According to Table 3, the soil glyphosate desorption results following a 0.1 M KH2PO4 treatment indicated a maximum desorption of 96.663% from soil C with the lowest sorption capacity, in agreement with Figure 5. A comparison of the recovery rates of glyphosate from all three applications is shown in Figure 5, with application 1 recovering the highest amount. Based on peak

recovery rates of glyphosate in soils A, B, and C, only 16.52%, 10.82%, and 22.40% for application 1; 3.98%, 1.58%, and 6.58% for application 2; and 9.58%, 5.93%, and 14.27% for application 3 were recovered. Due to glyphosate's low vapour pressure of 9.3×10^{-3} MPa (at 25 °C), its loss cannot be attributed to volatilization from the surface. Studies conducted under laboratory and outdoor conditions indicate that the loss of >40% after 118 days can be attributed to glyphosate mineralization into $^{14}CO_2$ [19].

Table 3. Glyphosate desorption from different soils.

Glyphosate Added, mg/L	Soils		
	Soil A (%)	Soil B (%)	Soil C (%)
5	89.233	87.668	96.663
10	84.052	88.780	80.071
12	92.709	87.349	84.708
15	95.006	83.557	76.873
20	87.019	82.844	83.853
22	86.896	79.864	79.387
25	94.343	77.286	70.593
5	89.233	87.668	96.663

Application 1　　　　　　　　　Application 2　　　　　　　　　Application 3
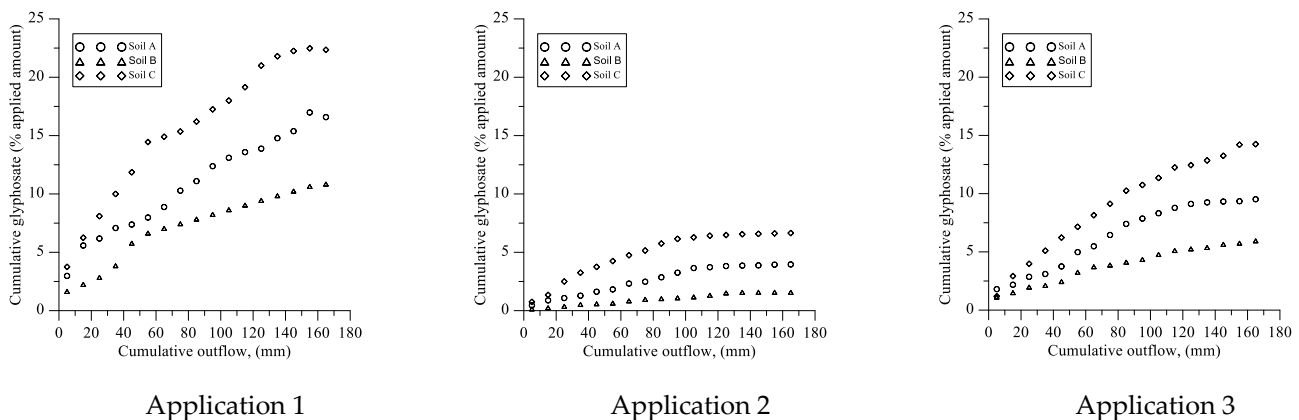
Figure 5. Percentage recovery of glyphosate from the three soil columns.

According to a previous study, glyphosate mineralization ($^{14}CO_2$) occurred within 42 days [19]. Using a two-chamber lysimeter test system, another study described mineralization in soil as glyphosate's primary elimination pathway and reported that over 50% of the radioactivity applied had been measured as $^{14}CO_2$ after 50 days [39]. Several other laboratory studies reported half-lives of less than 100 days for glyphosate [8,14,40,41].

The average half-life of glyphosate for first-order kinetics has been calculated by using the dissipation rates obtained from the HYDRUS 1D simulation by using an inverse modelling technique to fit the model solution to the observed data:

$$t_{1/2} = \frac{0.693}{\mu} \qquad (5)$$

3.4. Estimated Parameters

The numerical simulation was conducted using only glyphosate application as a pulse input, since the effluent concentrations of glyphosate were higher in application 1 than in the other two applications. Based on the results obtained using HYDRUS-1D, both equilibrium and non-equilibrium one-site sorption models accurately described glyphosate transport in a loam soil. To describe the data using the equilibrium model, the parameters derived from the batch sorption experiments were $K_f = 49.49 \text{ mg}^{1-(1/n)} \text{L}^n \text{kg}^{-1}$ and $1/n = 0.6289$ for soil A,

$K_f = 76.71$ mg$^{1-(1/n)}$L^{n}kg^{-1} and $1/n = 0.7350$ for soil B, and $K_f = 39.53$ mg$^{1-(1/n)}$L^{n}kg^{-1} and $1/n = 0.7400$ for soil C. The fitting of this equilibrium model (Figure 6) to the experimental data, taking K_f and $1/n$ as free adjustable parameters, compared well with the results obtained using the parameters in Table 4.
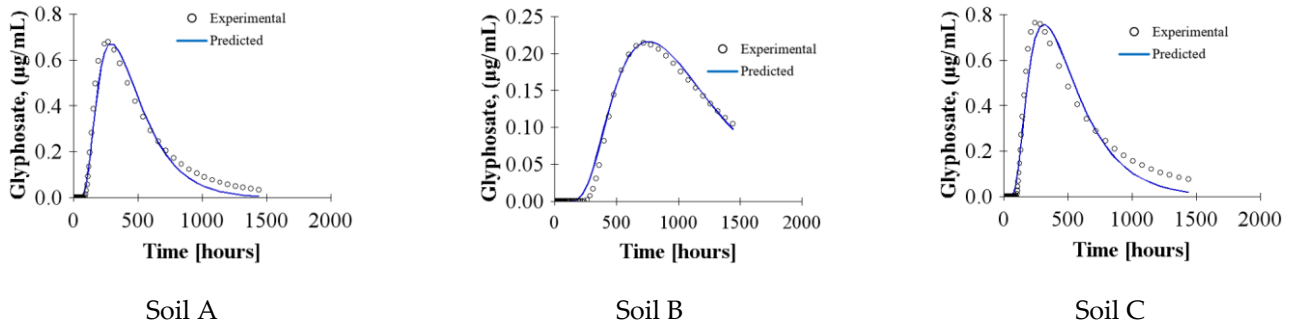

Figure 6. Glyphosate BTCs fitted with equilibrium model.

Table 4. The estimation of parameters for the glyphosate BTCs based on equilibrium models.

Soil Column	Half-Life, $t_{1/2}$ (Days)	RMSE [a]	R^2	K_f (mg$^{1-(1/n)}$L^{n}kg^{-1})	1/n(-)	α_k (h^{-1})	μ (h^{-1})
Soil A	57.000	0.014	0.968	37.210	1.000	0.180	0.397
Soil B	42.000	0.009	0.991	74.713	1.000	0.800	0.449
Soil C	46.000	0.013	0.979	34.633	1.000	0.100	0.516

[a] = root mean square error.

Furthermore, the glyphosate BTCs were well described by a fully kinetic, one-site, convective–dispersive model with degradation and Freundlich kinetic sorption; fitting parameters (Figure 7) are provided in Table 5. According to Tables 4 and 5, both models fit the glyphosate transport experimental data well. Both equilibrium and one-site sorption models showed lower Freundlich coefficients than batch experiments. The sorptions estimated from the column experiments often being lower than those estimated from the batch experiments can be explained as the rate of lateral diffusion of the sorbate to sorbent being limited by the advective transport [40], which was not considered in the batch experiments. Also, batch experiments were susceptible to limitations that could limit their transferability to field conditions, such as particle breakup during shaking, which led to larger sorption capacities and low soil-to-solution ratios. [41]. In addition, because the sorption of glyphosate decreases with increasing pH and decreasing ionic strength, as the pH value was increased in the column-leaching experiments, the sorption of glyphosate could have decreased [4,6,9].
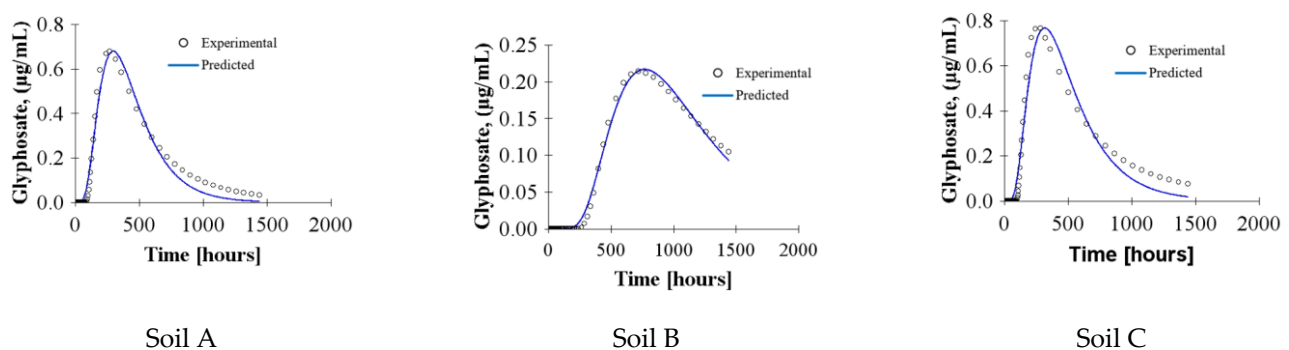

Figure 7. Glyphosate BTCs fitted with one-site sorption model.

Table 5. The estimation of parameters for the glyphosate BTCs based on one-site sorption model.

Soil Column	Half-Life, $t_{1/2}$ (Days)	RMSE [a]	K_f $(mg^{1-(1/n)}L^n kg^{-1})$	1/n(-)	α_k (h^{-1})	μ (h^{-1})	R^2
Soil A	42.000	0.016	34.547	1.009	0.694	0.294	0.958
Soil B	37.000	0.006	74.460	1.001	1.620	0.406	0.996
Soil C	33.000	0.015	30.724	1.005	0.383	0.365	0.972

[a] = root mean square error.

4. Discussion

In application 1, breakthroughs of the glyphosate occurred after 100, 312, and 103 h, respectively. It was observed that soil column C showed the greatest glyphosate breakthrough at a peak of 0.7627 g/mL, which was in agreement with the fact that soil C has a lower capacity for sorption than soils A and B. Application 2 had comparatively lower glyphosate concentrations than application 1, with first arrivals in soils A, B, and C occurring at 205 h, 328 h, and 168 h, respectively. Based on the results obtained from glyphosate application 3, it was difficult to determine whether phosphorus in the pre-saturation solution contributed to glyphosate leaching.

Based on the results of the three soils, soil B has a lower effluent glyphosate concentration, which could be due to (1) lower bromide breakthrough concentrations, (2) lower pH values, or (3) greater electrical conductivity. These factors indicate that soil B had a lower pore-water velocity than soils A and C, which subsequently resulted in lower glyphosate effluent concentrations. The recovery rates of the applied glyphosate for all three applications revealed that, considering the peak recovery rates of glyphosate, only 16.52%, 10.82%, and 22.4% were recovered from soils A, B, and C using application 1, while only 3.98%, 1.58%, and 6.58% were recovered from soils A, B, and C, respectively, using application 2. According to previous studies, glyphosate mineralization to $^{14}CO_2$ accounts for most of the loss.

5. Conclusions

Using glyphosate-dosed soils, column-leaching experiments were conducted with non-reactive tracer bromide combined with application and flow rates that mimicked field conditions. This study incorporated an experimental setup, with different glyphosate application scenarios, considering soil–glyphosate contact time variations and supposing a phosphate accumulation.

Miscible displacement experiments using glyphosate and non-reactive tracer bromide were modelled with HYDRUS-1D, a one-dimensional transport model. For the pulse boundary condition at the upper end and zero-gradient condition at the lower end, the analytical solution to the advection–dispersion equations (ADEs) was fitted to the experimental bromide breakthrough curves (BTCs). These parameters were then used in HYDRUS 1D to describe glyphosate's transport behaviour. This study describes the glyphosate transport using a convective–dispersive, fully kinetic, one-site model with degradation and Freundlich kinetic sorptions as well as a chemical equilibrium model.

6. Insights for Future Research

- Due to the fact that the leaching experiments carried out in this study considered soil depths up to only 20 cm, it would be more appropriate to conduct additional leaching experiments on this agricultural land for soil depths exceeding 1 m.
- A complete health risk assessment is needed on this agricultural land as a result of the fate of glyphosate and AMPA.
- Considering that this study only models 1D glyphosate transport, further modelling using 2D/3D cases is recommended.

References

1. Baylis, A.D. Why glyphosate is a global herbicide: Strengths, weaknesses and prospects. *Pest Manag. Sci.* **2000**, *56*, 299–308. [CrossRef]
2. Zhao, B.; Zhang, J.; Gong, J.; Zhang, H.; Zhang, C. Glyphosate mobility in soils by phosphate application: Laboratory column experiments. *Geoderma* **2009**, *149*, 290–297. [CrossRef]
3. Sprankle, P.; Meggitt, W.F.; Penner, D. Adsorption, mobility, and microbial degradation of glyphosate in the soil. *Weed Sci.* **1975**, *23*, 229–234. [CrossRef]
4. McConnell, J.S.; Hossner, L.R. pH-Dependent adsorption isotherms of glyphosate. *J. Agric. Food Chem.* **1985**, *33*, 1075–1078. [CrossRef]
5. Glass, R.L. Adsorption of glyphosate by soils and clay minerals. *J. Agric. Food Chem.* **1987**, *35*, 497–500. [CrossRef]
6. Nicholls, P.H.; Evans, A.A. Sorption of lonisable organic compounds by field soils. Part 2: Cations, bases and zwitterions. *Pestic. Sci.* **1991**, *33*, 331–345. [CrossRef]
7. Piccolo, A.; Celano, G.; Arienzo, M.; Mirabella, A. Adsorption and desorption of glyphosate in some European soils. *J. Environ. Sci. Health Part B* **1994**, *B29*, 1105–1115. [CrossRef]
8. Cheah, U.B.; Kirkwood, R.C.; Lum, K.Y. Adsorption, desorption and mobility of four commonly used pesticides in malaysian agricultural soils. *Pestic. Sci.* **1997**, *50*, 53–63. [CrossRef]
9. Jonge, H.d.; Jonge, L.W.d. Influence of pH and solution composition on the sorption of glyphosate and prochloraz to a sandy loam soil. *Chemosphere* **1999**, *39*, 753–763. [CrossRef]
10. Broster, J.C.; Jalaludin, A.; Widderick, M.J.; Chambers, A.J.; Walsh, M.J. Herbicide Resistance in Summer Annual Weeds of Australia's Northern Grains Region. *Agronomy* **2023**, *13*, 1862. [CrossRef]
11. Venâncio, C.; Barbosa, C.; Lopes, I. Glyphosate and Roundup® Ready Effects in Hydra viridissima: New Data in an Old Issue. *Sustainability* **2023**, *15*, 12428. [CrossRef]
12. Malmo, A.; Broster, J.C.; Walsh, M.J. Looking beyond Glyphosate for Site-Specific Fallow Weed Control in Australian Grain Production. *Agronomy* **2023**, *13*, 1878. [CrossRef]
13. Jonge, H.d.; Jonge, L.W.d.; Jacobsen, O.H.; Yamaguchi, T.; Moldrup, P. Glyphosate sorption in soils of different pH and phosphorous content. *Soil Sci.* **2001**, *166*, 230–238. [CrossRef]
14. Borggaard, O.K.; Gimsing, A.L. Fate of glyphosate in soil and the possibility of leaching to ground and surface waters: A review. *Pest Manag. Sci.* **2008**, *64*, 441–456. [CrossRef]
15. Kisvarga, S.; Hamar-Farkas, D.; Horotán, K.; Inotai, K.; Mörtl, M.; Neményi, A.; Székács, A.; Orlóci, L. Morphological, Histological, and Glyphosate Residue Analysis of Helianthus annuus L. Plants Treated with Glyphosate. *Agriculture* **2023**, *13*, 1014. [CrossRef]
16. Kanissery, R.; Gairhe, B.; Kadyampakeni, D.; Batuman, O.; Alferez, F. Glyphosate: Its environmental persistence and impact on crop health and nutrition. *Plants* **2019**, *8*, 499. [CrossRef] [PubMed]
17. Veiga, F.; Zapata, J.M.; Marcos, M.L.F.; Alvarez, E. Dynamics of glyphosate and aminomethylphosphonic acid in a forest soil in Galicia, north-west Spain. *Sci. Total Environ.* **2001**, *271*, 135–144. [CrossRef] [PubMed]
18. Kjaer, J.; Olsen, P.; Ullum, M.; Grant, R. Leaching of glyphosate and amino-methylphosphonic acid from danish agricultural field sites. *J. Environ. Qual.* **2005**, *34*, 608–620. [CrossRef]
19. Landry, D.; Dousset, S.; Fournier, J.-C.; Andreux, F. Leaching of glyphosate and AMPA under two soil management practices in Burgundy vineyards. *Environ. Pollut.* **2005**, *138*, 191–200. [CrossRef]
20. Mertens, M.; Höss, S.; Neumann, G.; Afzal, J.; Reichenbecher, W. Glyphosate, a chelating agent—Relevant for ecological risk assessment? *Environ. Sci. Pollut. Res.* **2018**, *25*, 5298–5317. [CrossRef]
21. Ortiz, A.M.G.; Okada, E.; Bedmar, F.; Costa, J.L. Sorption and desorption of glyphosate in Mollisols and Ultisols soils of Argentina. *Environ. Toxicol. Chem.* **2017**, *36*, 2587–2592. [CrossRef] [PubMed]
22. Padilla, J.T.; Selim, H.M. Glyphosate Transport in Two Louisiana Agricultural Soils: Miscible Displacement Studies and Numerical Modeling. *Soil Syst.* **2018**, *2*, 53. [CrossRef]
23. Gimsing, A.L.; Borggaard, O.K.; Bang, M. Influence of soil composition on adsorption of glyphosate and phosphate by contrasting Danish surface soils. *Eur. J. Soil Sci.* **2004**, *55*, 183–191. [CrossRef]

24. Strange-Hansen, R.; Holm, P.E.; Jacobsen, O.S.; Jacobsen, C.S. Sorption, mineralization and mobility of N-(phosphonomethyl)glycine (glyphosate) in five different types of gravel. *Pest Manag. Sci.* **2004**, *60*, 570–578. [CrossRef] [PubMed]

25. Torstensson, L.; Börjesson, E.; Stenström, J. Efficacy and fate of glyphosate on Swedish railway embankments. *Pest Manag. Sci.* **2005**, *61*, 881–886. [CrossRef] [PubMed]

26. Miyano, H.; Toyo'oka, T.; Imai, K.; Nakajima, T. Influences of metal ions on the reaction of amino and imino acids with fluorogenic reagents. *Anal. Biochem.* **1985**, *150*, 125–130. [CrossRef] [PubMed]

27. Nahar, K. *A Low Cost Method for Glyphosate Analysis, and Site Investigation and Modelling of Glyphosate Fate and Transport from Genetically Modified Canola Farmland in Parkes, NSW, Australia*; UNSW Sydney: Sydney, Australia, 2015.

28. Gimsing, A.L.; Borggaard, O.K. Effect of KCl and $CaCl_2$ as background electrolytes on the competitive adsorption of glyphosate and phosphate on geothite. *Clays Clay Miner.* **2001**, *49*, 270–275. [CrossRef]

29. Autio, S.; Siimes, K.; Laitinen, P.; Rämö, S.; Oinonen, S.; Eronen, L. Adsorption of sugar beet herbicides to Finnish soils. *Chemosphere* **2004**, *55*, 215–226. [CrossRef]

30. Gimsing, A.L.; Borggaard, O.K. Competitive adsorption and desorption of glyphosate and phosphate on clay silicates and oxides. *Clay Miner.* **2002**, *37*, 509–515. [CrossRef]

31. Gimsing, A.L.; Szilas, C.; Borggaard, O.K. Sorption of glyphosate and phosphate by variable-charge tropical soils from Tanzania. *Geoderma* **2007**, *138*, 127–132. [CrossRef]

32. Attaallah, M.A. The Kinetic Study of Glyphosate Leachate in Palestinian Soil at Different Concentrations. Master's Thesis, An-Najah National University, Nablus, Palestine, 2011.

33. Gerritse, R.G.; Beltran, J.; Hernandeg, F. Adsorption of atrazine, simazine, and glyphosate in soils of the Gnangara Mound, Western Australia. *Aust. J. Soil Res.* **1996**, *34*, 599–607. [CrossRef]

34. Wang, Y.J.; Zhou, D.M.; Sun, R.J. Effects of phosphate on the adsorption of glyphosate on three different types of Chinese soils. *J. Environ. Sci.* **2005**, *17*, 711–715.

35. *Fate, Transport and Transformation Test Guidelines*; United States Environmental Protection Agency: Washington, DC, USA, 2008.

36. Toride, N.; Leij, F.J.; van Genuchten, M.T. *The CXTFIT Code for Estimating Transport Parameters from Laboratory or Field Tracer Experiments*; U.S. Department of Agriculture: Riverside, CA, USA, 1995.

37. Grundmann, S.; Dörfler, U.; Ruth, B.; Loos, C.; Wagner, T.; Karl, H.; Munch, J.C.; Schroll, R. Mineralization and transfer processes of 14C-labeled pesticides in outdoor lysimeters. *Water Air Soil Pollut.* **2008**, *8*, 177–185. [CrossRef]

38. Gimsing, A.L.; Borggaard, O.K.; Jacobsen, O.S.; Aamand, J.; Sørensen, J. Chemical and microbiological soil characteristics controlling glyphosate mineralisation in Danish surface soils. *Appl. Soil Ecol.* **2004**, *27*, 233–242. [CrossRef]

39. Nomura, N.S.; Hilton, H.W. The adsorption and degradation of glyphosate in five Hawaiian sugarcane soils. *Weed Res.* **2006**, *17*, 113–121. [CrossRef]

40. Casey, F.X.M.; Hakk, H.; Šimůnek, J.; Larsen, G.L. Fate and transport of testosterone in agricultural soils. *Environ. Sci. Technol.* **2004**, *38*, 790–798. [CrossRef] [PubMed]

41. Buergisser, C.S.; Cernik, M.; Borkovec, M.; Sticher, H. Determination of nonlinear adsorption isotherms from column experiments: An alternative to batch studies. *Environ. Sci. Technol.* **1993**, *27*, 943–948. [CrossRef]